Quantitative Image Reconstruction of GaN Quantum Dots from Oversampled Diffraction Intensities Alone

Jianwei Miao,[1] Yoshinori Nishino,[2] Yoshiki Kohmura,[2] Bart Johnson,[3] Changyong Song,[1] Subhash H. Risbud,[4] and Tetsuya Ishikawa[2]

[1]*Department of Physics and Astronomy and CNSI, University of California, Los Angeles, California 90095-1547, USA*
[2]*SPring-8/RIKEN, 1-1-1, Kouto, Mikazuki, Sayo-gun, Hyogo 679-5198, Japan*
[3]*Stanford Synchrotron Radiation Laboratory, Stanford Linear Accelerator Center, Menlo Park, California 94025, USA*
[4]*Department of Chemical Engineering and Materials Science, University of California, Davis, California 95616, USA*
(Received 8 March 2005; published 17 August 2005)

The missing data problem, i.e., the intensities at the center of diffraction patterns cannot be experimentally measured, is currently a major limitation for wider applications of coherent diffraction microscopy. We report here that, when the missing data are confined within the centrospeckle, the missing data problem can be reliably solved. With an improved instrument, we recorded 27 oversampled diffraction patterns at various orientations from a GaN quantum dot nanoparticle and performed quantitative image reconstruction from the diffraction intensities alone. This work in principle clears the way for single-shot imaging experiments using x-ray free electron lasers.

DOI: 10.1103/PhysRevLett.95.085503 PACS numbers: 61.10.Nz, 42.30.Rx, 42.30.Wb

The discovery and interpretation of x-ray diffraction in crystals by M. van Laue, W. H. Bragg, and W. L. Bragg in the early 20th century opened up a new era for visualizing the arrangement of atoms in three dimensions. Indeed, x-ray crystallography has since made revolutionary impacts in a number of fields ranging from physics, materials sciences, and chemistry to biology. It, however, requires high quality and sizable crystals, and the 3D structure determined is globally averaged from a large number of identical copies. It was not until recently that the key requirement in x-ray crystallography (i.e., crystallinity) was released by using coherent diffraction microscopy [1], which records a coherent diffraction pattern from a noncrystalline specimen or a small crystal and performs the direct phase recovery from the diffraction intensities by using the oversampling method. Coherent diffraction microscopy has since been used to image materials and biological systems in both two and three dimensions [1–16]. A highest resolution of 7 nm has been achieved with x rays [14] and 1 Å with electrons [10]. While significant progress has been made during the past few years, a major obstacle still remains to be overcome (i.e., the missing data problem). This is because, in recording a diffraction pattern, the central intensities are mixed with the direct beam and have to be blocked by a beamstop. As the central intensities correspond to the lower spatial frequency of the sample structure, their absence makes the direct phase retrieval difficult and sometimes impossible. The conventional solution is to calculate the missing central intensities from a lower resolution image of an x-ray or electron microscope [17]. This process, however, not only is extremely inconvenient for 3D imaging and makes it impossible to study the dynamics of materials, but also introduces artifacts in the reconstructed images due to the different contrast mechanism between lens-based microscopy and coherent different microscopy. Furthermore, single-shot imaging experiments using x-ray free electron lasers would be impossible without solving the missing data problem as each specimen may be destroyed after a single pulse [3,18]. Although more sophisticated algorithms have been developed to deal with the missing data problem [7,15], they do not work for general samples. This is because, when the missing data size is larger than the centrospeckle, some structural information about the specimen is permanently lost and cannot be recovered by using iterative algorithms. In this Letter, we report a general approach to perform image reconstruction from oversampled diffraction intensities alone. By using an improved coherent diffraction microscope, we recorded 27 oversampled diffraction patterns by rotating a GaN quantum dot particle around a single axis with the missing data confined within the centrospeckle. Quantitative images were directly reconstructed from the oversampled diffraction patterns alone.

When a coherent wave illuminates an isolated specimen, the far-field diffraction intensities are continuous. The continuous intensities can be sampled at an arbitrary frequency. When the sample frequency is sufficiently finer than the Nyquist interval so that the number of correlated intensity points is more than the number of unknown variables, the phases are, in principle, uniquely encoded in the intensities [19] and can be directly retrieved by using an iterative algorithm [20]. Here the number of unknown variables represents the voxel number of an array sampling the structure of the specimen. The oversampling ration (σ) was used to characterize the degree of oversampling where $\sigma = \sigma_x \sigma_y \sigma_z$ and σ_x, σ_y, σ_z represent the sampling frequency divided by the Nyquist interval in the X, Y, and Z

 © 2005 The American Physical Society

directions [19]. When $\sigma > 2$, the number of correlated intensity points is more than the number of unknown variables.

For an isolated sample, its oversampled diffraction pattern consists of a series of speckles where the speckle size is proportional to the inverse of the sample size. Since the intensity information within each speckle corresponds to a real-space dimension larger than the sample size, phase retrieval from oversampled diffraction intensities is sensitive only to the number of missing speckles instead of the number of missing pixels. We characterize the number of missing speckles by

$$\eta_i = \frac{D_i - 1}{2\sigma_i}, \qquad i = x, y, z, \tag{1}$$

where η_i is called the number of missing waves and D_i the number of missing pixels. As the speckles at the center correspond to the lower spatial frequencies, the missing speckles cause density oscillation in real space and the oscillation wavelength is determined by η_i [21]. We performed simulations to illustrate the effect of the number of missing waves on phase retrieval, shown in Fig. 1. We calculated an oversampled diffraction pattern from a 128×128 pixel image with σ_x and $\sigma_y = 4$. Intensities were removed from the center of the diffraction pattern with η_x and $\eta_y = 1$, 2, and 4, respectively. We carried out reconstruction of the oversampled diffraction patterns by using an iterative algorithm. The algorithm first generated an initial random phase set. In combination of the random phase set with the square root of the diffraction intensities, a reciprocal-space complex array was obtained. By applying inverse fast-Fourier transform (FFT) to the complex array, a real-space complex array was created. The real part of the real-space array corresponds to the electron density of the specimen, and the imaginary part was set to zero. A support was defined to separate the electron density from the no-density region, whereas the no-density region is due to oversampling of the diffraction intensities. The electron density outside the support and the negative electron density inside the support were slowly pushed to zero. By applying FFT to the modified real-space array, an updated reciprocal-space array was obtained. The modulus of the updated reciprocal-space array was replaced with the square root of the diffraction intensities, whereas the modulus within the missing data area was kept unchanged. This process created a new reciprocal-space array, which was used for the next iteration. In the reconstruction of Fig. 1, we have tried both a tight and a loose support, whereas the tight support is a 128×128 pixel square (i.e., the true envelope of the specimen) and the loose support is a 138×138 pixel square. For each support, we conducted five trials with different initial random phase sets. The reconstructed images were consistent with both supports, while the convergence speed of using the tight support was faster than that of the loose support. Figure 1 shows the reconstructions after 1000 iterations by using the tight support and the same initial seed. A real-space R factor was used to characterize the reconstructions, defined as $R_{\text{real}} = \sqrt{\sum(\rho_{\text{orig}} - \rho_{\text{rec}})^2 / \sum(\rho_{\text{orig}} + \rho_{\text{rec}})^2}$, where ρ_{orig} and ρ_{rec} represent the original and reconstructed image. R_{real} is 0.03%, 1.6%, and 13.2% for Figs. 1(a)–1(c), respectively. The reconstructed image was almost perfect with η_x and $\eta_y = 1$, shown in Fig. 1(a). This is because the data within the centrospeckle determine only a scaling factor of the electron density of the specimen, and does not carry any structural information. Although it is not obvious in Fig. 1(b), density oscillation starts to appear inside the reconstructed image when η_x and $\eta_y = 2$ as indicated by R_{real}. Oscillation becomes obvious when η_x and $\eta_y = 4$, shown in Fig. 1(c). The simulations demonstrated that, when η_x and $\eta_y > 1$, some structural information about the sample is permanently lost, which introduces artifacts in the reconstructed images. The missing structural information cannot be recovered by iterative algorithms no matter whether a tight support is used [7] or the center pixel in the reciprocal-space array is fixed [15]. To reliably solve the missing data problem for general samples, one needs to obtain oversampled diffraction patterns with the missing data confined within the centrospeckle.

To experimentally verify this conclusion, we modified our existing coherent x-ray diffraction microscope [14] to record oversampled diffraction patterns with the missing data inside the centrospeckle. Figure 2 shows a schematic layout of the modified microscope, mounted on an undulator beam line with 5 keV x rays. The spectral resolution ($\lambda/\Delta\lambda$) and the divergence angle of the beam are $\sim$7500 and $\sim 10^{-5}$ rad, respectively. The first element inside the microscope was a 30 μm pinhole used for generating a plane wave illumination and reducing the size of the illumination area. At a distance of 54 cm downstream of the pinhole was a silicon window with beveled edges, acting as

FIG. 1. Image reconstruction of oversampled diffraction patterns as a function of the number of missing waves. (a) η_x, $\eta_y = 1$. (b) η_x, $\eta_y = 2$. (c) η_x, $\eta_y = 4$.

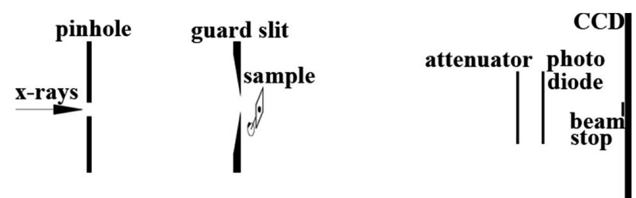

FIG. 2. A schematic layout of an instrument for recording oversampled diffraction patterns with the missing data confined within the centrospeckle.

a guard slit to remove the scattering from the pinhole. The sample, supported on a 30 nm thick Si_3N_4 membrane, was mounted immediately after the guard slit and can be rotated around one axis. A CCD detector was placed downstream of the sample with an adjustable distance from 86.6 to 112 cm. The longer distance was to increase the oversampling ratio and reduce η_x and η_y. An attenuator and a photodiode can be inserted in the optical path for aligning the optical elements. A beamstop was positioned very close to the CCD detector to block the direct beam. All the elements were in vacuum with a pressure of $\sim 10^{-6}$ torr. This modification allowed us to record oversampled diffraction patterns from general micron-sized samples with the missing data confined within the centrospeckle.

The sample is GaN particles commercially obtained from Atomergic Chemicals Corp. Atomic force microscopy (AFM) images of the as-received particles show the morphology of platelike structures with an averaged length about 230 nm [Fig. 3(a)] and the aggregation of these plates to form agglomerates. The GaN particles with high purity and low oxygen content were heat treated at 900 °C for 1 h in a flowing stream of N_2 gas (flow rate of 100 ml/min). Routine x-ray diffraction, electron microscopy, and ^{71}Ga solid state NMR data showed that the heat-treated GaN powders were oxidized at the surface to β-Ga_2O_3 leaving behind nanosize GaN quantum dot cores [22]. High-resolution TEM images showed lattice fringes from the GaN quantum dots (varying in size from 2.5 to 7 nm) [22]. The quantum dot particles were dispersed in pure ethanol and deposited on 30 nm thick silicon nitride membranes. The well-isolated particles with appropriate sizes were chosen by using a light microscope. Figure 3(b) shows a scanning electron microscopy (SEM) image of a GaN particle used for the x-ray diffraction experiment.

A series of 27 oversampled diffraction patterns was experimentally recorded by rotating the GaN particle around a single axis ranging from $-69.4°$ to $+69.4°$. The rotation angles were chosen such that projections are equally sloped instead of equally angled, which can make better 3D reconstruction [23]. Each diffraction pattern has 800×800 pixels with the missing data confined within the centrospeckle (i.e., η_x and $\eta_y \leq 1$). Figure 3(c) shows the central part (512×512 pixel) of the diffraction pattern with the rotation angle at 0°, in which the square (29×29 pixels) at the center represents the missing data. The iterative algorithm described above was used to retrieve the phases of the 27 oversampled diffraction patterns. To reduce the reconstruction error, we carried out ten trials for each diffraction pattern with different initial seeds and characterized them by using $R_{ij} = \sqrt{\sum(\rho_i - \rho_j)^2 / \sum(\rho_i + \rho_j)^2}$, where i and j represent the ith and jth trials. Based on R_{ij}, we chose the five best reconstructed images out of ten for each diffraction pattern and averaged them to obtain a final one. Figure 4 shows the final images reconstructed from the diffraction patterns with the rotation angles ranging from 0° to 69.4° (the other 13 final images with the angles ranging from $-7.1°$ to $-69.4°$ are not shown) of which the rotation axis is indicated in Fig. 4(a). An averaged R_{ij} of five best trials for each final image was calculated to be between 5.58% and 7.29%. The small averaged R_{ij} indicates the robustness of the reconstructions.

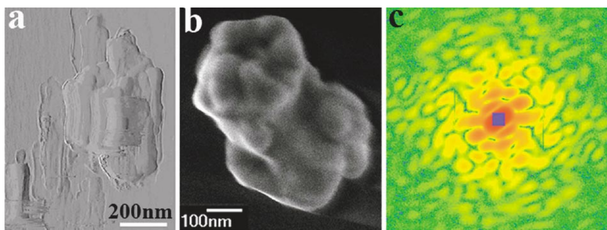

FIG. 3 (color). (a) An AFM image of as-received GaN quantum dot particles. (b) An SEM image of the GaN quantum dot particle used for the x-ray diffraction experiment. The image was taken after the x-ray experiment. Note that (a) and (b) are not the same GaN particle. (c) The oversampled diffraction pattern with the rotation angle at 0°.

While the reconstructed image at 0° angle [Fig. 4(a)] resembles the SEM image [Fig. 3(b)], it provides different structural information. This is because Fig. 4(a) shows a quantitative projection of the GaN particle and Fig. 3(b) shows only the surface morphology. For example, the darker region in Fig. 4(a) representing the higher electron density is due to the 3D morphology of the particle, which cannot be deduced from Fig. 3(b). Careful examination of the reconstructed images reveals the morphology of platelike structures, which are indicated by arrows in Figs. 4(e)–4(m). The platelet length is about 230 nm (see the scale bar in Fig. 4(i)], which is consistent with the AFM image shown in Fig. 3(a). As the resolution of the reconstructed images (~ 30 nm) is lower than the lattice spacing for both GaN and Ga_2O_3, the GaN-Ga_2O_3 core-shell structures are indistinguishable in these images. The ultimate resolution of coherent diffraction microscopy, however, is limited only by the x-ray wavelength. By using brighter x-ray sources and better detector systems, near atomic resolution will be achievable for radiation hard materials, as there are no further fundamental obstacles for the imaging technique. The quantitative image reconstruction from oversampled diffraction patterns alone will likely have an important impact in nanoscience and technology for 3D characterization of materials and biological systems. For example, as a nondestructive imaging technique, coherent diffraction microscopy can be applied to image buried structures and interfaces, study the dynamics of materials, and visualize the 3D distribution of strains, defects, and deformation structures. As the reconstruction artifacts are greatly reduced by setting η_x and $\eta_y \leq 1$, fine density variations such as two materials with similar densities can be distinguished by this imaging technique. Furthermore, it can be applied to perform 3D elemental and chemical mapping of materials and biological systems by tuning

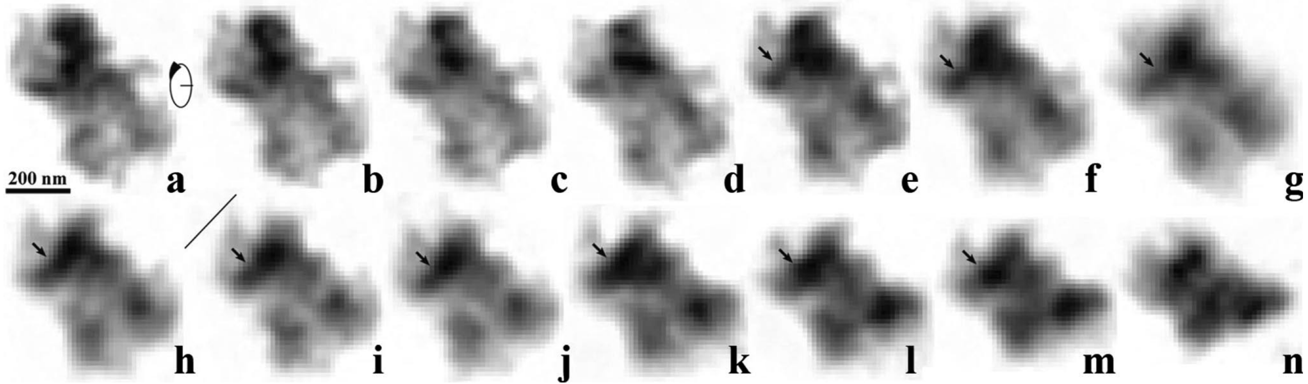

FIG. 4. Quantitative image reconstruction of the GaN quantum dot particle from oversampled diffraction patterns alone. The rotation angle and the averaged R_{ij} are (a) 0° and 5.85%, (b) 7.1° and 7.05%, (c) 14° and 5.98%, (d) 20.6° and 6.75%, (e) 26.6° and 6.27%, (f) 32° and 5.66%, (g) 36.9° and 6.28%, (h) 41.2° and 7.29%, (i) 45° and 6.37%, (j) 48.8° and 6.26%, (k) 53.1° and 5.58%, (l) 58° and 7.06%, (m) 63.4° and 5.98%, (n) 69.4° and 6.14%. The scale bar in (i) is 230 nm.

the x-ray wavelength to a specific absorption edge and recording diffraction patterns above and below the edge.

We have shown that phase retrieval of oversampled diffraction intensities is sensitive only to the number of missing speckles instead of the number of missing pixels. The number of missing waves (η_x and η_y) was introduced to characterize the missing data. When η_x and $\eta_y > 1$, some structural information about the specimen is permanently lost, which causes density oscillation in the real-space image. When η_x and $\eta_y \leq 1$, i.e., the missing data are confined within the centrospeckle, phases can be reliably retrieved from oversampled diffraction patterns alone. With an improved coherent x-ray diffraction microscope, we demonstrated that oversampled diffraction patterns can be obtained from very general samples with the missing data confined within the centrospeckle. We recorded 27 diffraction patterns by rotating a GaN quantum dot particle around a single axis. Quantitative images were reconstructed from the oversampled diffraction patterns alone. We believe this very general approach will have a broad impact in 3D characterization of materials and biological systems. Furthermore, this work will make single-shot imaging experiments possible by using x-ray free electron lasers, which are currently under rapid development worldwide.

We thank D. Durkin and K. O. Hodgson for many stimulating discussions, as well as M. Yabashi and K. Tamasaku for the help of data acquisition. This work was supported by the U.S. Department of Energy, Office of Basic Energy Sciences. Use of the RIKEN beam line (BL29XUL) at SPring-8 was supported by RIKEN.

[1] J. Miao, P. Charalambous, J. Kirz, and D. Sayre, Nature (London) **400**, 342 (1999).
[2] I. K. Robinson and J. Miao, MRS Bull. **29**, 177 (2004).
[3] J. Miao *et al.*, Annu. Rev. Biophys. Biomol. Struct. **33**, 157 (2004).
[4] I. K. Robinson *et al.*, Phys. Rev. Lett. **87**, 195505 (2001).
[5] J. Miao *et al.*, Phys. Rev. Lett. **89**, 088303 (2002).
[6] H. He *et al.*, Phys. Rev. B **67**, 174114 (2003).
[7] S. Marchesini *et al.*, Phys. Rev. B **68**, 140101 (2003).
[8] K. A. Nugent *et al.*, Phys. Rev. Lett. **91**, 203902 (2003).
[9] G. J. Williams *et al.*, Phys. Rev. Lett. **90**, 175501 (2003).
[10] J. M. Zuo *et al.*, Science **300**, 1419 (2003).
[11] S. Eisebitt *et al.*, Appl. Phys. Lett. **84**, 3373 (2004).
[12] W. McBride, N. L. O'Leary, and L. J. Allen, Phys. Rev. Lett. **93**, 233902 (2004).
[13] H. M. L. Faulkner and J. M. Rodenburg, Phys. Rev. Lett. **93**, 023903 (2004).
[14] J. Miao *et al.*, Phys. Rev. B **67**, 174104 (2003).
[15] Y. Nishino, J. Miao, and T. Ishikawa, Phys. Rev. B **68**, 220101 (2003).
[16] V. Elser, Acta Crystallogr. Sect. A **59**, 201 (2003).
[17] For small crystals, another solution to the missing data problem is based on Bragg diffraction pioneered by Robinson *et al.* [4,9] where a Bragg peak and its adjacent intensities are oversampled and the phases are retrieved by an iterative algorithm. The reconstructed image reveals the defects, strains, and grain boundary of the lattice, but not the electron density or charge potential of the samples.
[18] R. Neutze *et al.*, Nature (London) **406**, 752 (2000).
[19] J. Miao, D. Sayre, and H. N. Chapman, J. Opt. Soc. Am. A **15**, 1662 (1998).
[20] J. R. Fienup, Opt. Lett. **3**, 27 (1978).
[21] To illustrate the density oscillation due to the missing speckles, we calculated a complex array (512×512 pixels) by Fourier transforming an image (128×128 pixels), where σ_x and $\sigma_y = 4$. The central 9×25 pixels of the complex array were set to zero (i.e., $\eta_x = 1$ and $\eta_y = 3$). By applying inverse FFT to the complex array, a real-space array was obtained in which the density oscillation was observed. Within the image area of 128×128 pixels, there are exactly one and three oscillation wavelengths in the X and Y directions, i.e., $\eta_x = 1$ and $\eta_y = 3$.
[22] J. Tong and S.H. Risbud, J. Solid State Chem. **177**, 3568 (2004).
[23] J. Miao, F. Förster, and O. Levi, Phys Rev. B (to be published).